

Received: 2020.02.20

Accepted: 2020.05.05

Available online: 2020.12.15

Published: 2021.02.19

# Ultrasound-Targeted Microbubble Destruction Enhances the Inhibitive Efficacy of miR-21 Silencing in HeLa Cells

Authors' Contribution:

Study Design A  
Data Collection B  
Statistical Analysis C  
Data Interpretation D  
Manuscript Preparation E  
Literature Search F  
Funds Collection G

**AE 1 Shengli Zhao\***  
**AB 2 Jing Xie\***  
**C 3 Changhua Zhao**  
**D 4 Wen Cao**  
**F 5 Yangping Yu**

1 Department of Ultrasonography, The Second People's Hospital of Liaocheng, Liaocheng, Shandong, P.R. China  
2 Department of Ultrasonography, Wucheng Traditional Chinese Medicine (TMC) Hospital, Wucheng, Shandong, P.R. China  
3 Department of Ultrasonography, Zhucheng People's Hospital, Zhucheng, Shandong, P.R. China  
4 Department of Oncology, Yidu Central Hospital of Weifang, Weifang, Shandong, P.R. China  
5 Department of Ultrasonography, Jining No. 1 People's Hospital, Jining, Shandong, P.R. China

**Corresponding Author:**

**Source of support:**

\* Shengli Zhao and Jing Xie contributed equally to this work

Yangping Yu, e-mail: [yangp\\_yuyp@163.com](mailto:yangp_yuyp@163.com)

Departmental sources

**Background:** Previous studies have shown that miR-21 upregulation is related to the aggressive development of cervical cancer. Ultrasound-targeted microbubble destruction (UTMD) is a method that increases the absorption of targeted genes or drugs by cells. We focus on the role of UTMD-mediated miR-21 transfection in HeLa cells, a cervical cancer cell line.

**Material/Methods:** The effects of different ultrasound intensities on the transfection efficiency of miR-21-enhanced green fluorescent protein (EGFP) and miR-21 inhibitor-EGFP plasmids were determined by flow cytometry. The effects of UTMD-mediated miR-21 transfection on HeLa cell proliferation, apoptosis, migration, and invasion were measured by CCK-8, flow cytometry, wound healing experiments, and transwell migration assay, respectively. Western blot and real-time quantitative PCR were used to detect the expression of tumor-related genes.

**Results:** When the ultrasound intensity was 1.5 W/cm<sup>2</sup>, the miR-21 plasmid had the highest transfection efficiency. Exogenous miR-21 promoted cell proliferation, migration, and invasion, and inhibited cell apoptosis in HeLa cells. Treatment of cells with UTMD further enhanced the effects of miR-21-EGFP and miR-21 inhibitor-EGFP. In addition, miR-21 overexpression significantly increased the expression of p-Akt, Akt, Bcl-2, Wnt, β-catenin, matrix metalloprotein-9 (MMP-9), and epidermal growth factor (EGFR) levels, and decreased Bax expression. The regulatory role of miR-21 inhibitor-EGFP was opposite to that of miR-21-EGFP. After UTMD, miR-21-EGFP and miR-21 inhibitor-EGFP had more significant regulatory effects on these genes.

**Conclusions:** Our research revealed that an ultrasound intensity of 1.5 W/cm<sup>2</sup> is the best parameter for miR-21 transfection. UTMD can enhance the biological function of miR-21 in HeLa cells, and alter the effect of miR-21 on apoptosis, metastasis, and phosphorylation genes.

**Keywords:** **Cell Proliferation • Microbubbles • Ultrasonography • Uterine Cervical Neoplasms**

Full-text PDF: <https://www.medscimonit.com/abstract/index/idArt/923660>

 3094

 —

 4

 36



## Background

Cervical cancer is a common gynecological malignant tumor; it is the second most common malignant tumor in women after breast cancer [1]. Although research on cervical cancer has made great breakthroughs, it is still a risk factor for serious adverse effects on the physical and mental health of women [2]. At present, the treatment of cervical cancer is mainly based on the stage and patient age, and comprehensive treatment, including surgery, radiotherapy, chemotherapy, vaccine, and other methods, is commonly applied [1,2]. For example, in the chemotherapy scheme of cervical cancer, combined chemotherapy based on cisplatin is mostly used [3]. Gynecological tumors are highly sensitive to platinum and it has good curative effects [4]. However, the toxic adverse effects of platinum and drug resistance are important factors affecting the application of platinum [4]. Despite continuous improvements in surgical techniques, radiotherapy equipment and technology, and emerging chemotherapeutic drugs, none have fundamentally improved patient survival [5,6].

Ultrasound-targeted microbubble destruction (UTMD) is a technology that can increase the absorption of targeted drugs by cells, thereby increasing the efficacy of drugs [7]. Perfluoropropane human serum albumin microsphere injection is a new type of second-generation ultrasound contrast agent in UTMD [8]. The main active ingredient is human serum albumin microspheres coated with octafluoropropane [7]. The technology mainly uses microbubbles to localize a “blast” using ultrasound irradiation to release the genes it carries [7,8]. At the same time, the shock caused by ultrasonic and microbubble rupture increases local cell permeability, generates reversible acoustic pores, and promotes the entry of genes into the nucleus, which can improve the transfection and expression efficiency of genes [9]. Secondly, the protection of microbubbles can prevent the carried genes or drugs from being degraded by the endonucleases in the plasma, so that they can stably reach the target organ or tissue through blood circulation [10]. Dimceviski and other scholars used conventional diagnostic ultrasound combined with ultrasound contrast agents to perform gemcitabine chemotherapy sensitization of pancreatic cancer and achieved certain therapeutic effects [11].

Clinical investigation revealed that miR-21 expression is significantly elevated in cervical cancer patients, and miR-21 up-regulation is related to the aggressive development of cervical cancer [12]. Reported studies have shown that increasing miR-21 expression can promote HeLa cell growth [13]. UTMD enhances gene expression of miR-21 in swine heart via intracoronary delivery [14]. However, the mechanism of the expression of miR-21 from UTMD-mediated transfection, and the parameters of different cells and tissues, need further study. In this study, the optimal intensity parameters for transfection

efficiency for UTMD-mediated miR-21 plasmid transfection in the HeLa cell line, which is derived from cells from cervical cancer patient Henrietta Lacks, were selected, and the effect of UTMD-mediated miR-21 transfection on HeLa cell biology was studied.

## Material and Methods

### Cell culture

HeLa cells were purchased from American Tissue Culture Collection (CCL-2, Gaithersburg, MD, USA). The cells were cultured in Dulbecco's modified Eagle's medium (DMEM; 12491015, Thermo Fisher Scientific, Waltham, MA, USA) with 10% fetal bovine serum (FBS, 30067334, Thermo Fisher Scientific, Waltham, MA, USA) and 1% penicillin-streptomycin (15140163, Thermo Fisher Scientific, Waltham, MA, USA) in a 37°C carbon dioxide cell incubator (5% CO<sub>2</sub>, BC-J160, Boxun, Shanghai, China). During the culture process, the DMEM medium was changed once every 2-3 days. When the cells were grown to 80-90% confluence, the cells need to be subcultured.

### Preparation of Microbubbles and Plasmid DNA, and Transfection with Ultrasonic Exposure

The expression of enhanced green fluorescent protein (EGFP) was assessed using flow cytometry to determine DNA transfection efficiency (the number of cells expressing EGFP per number of cells in total). The miR-21-EGFP and miR-21 inhibitor-EGFP plasmids were purchased from RIBOBIO Company (Guangzhou, China). Perfluoropropane albumin microsphere injection (PFPAM) (S2008309, Jingda Pharmaceutical Co., Ltd., Guangzhou, China) was used in this experiment. PFPAM contains 5.18-6.08×10<sup>8</sup> microbubbles per milliliter. According to the manufacturer's instructions, we mixed JetPEI (PT-101-10N, Polyplus, Strasbourg, France) and miR-21-EGFP or miR-21 inhibitor-EGFP in a volume ratio of 2: 1 in 150 mM NaCl and then we incubated the mixture at room temperature for 20 minutes. Then, the plasmid DNA and PFPAM were slowly mixed in Opti-MEM (31985070, Invitrogen, Carlsbad, CA, USA) to a final volume of 500 μL to form a transfection complex. The transfection complexes were incubated for 15 min before being used for transfection.

Prior to the experiment, HeLa cells were cultured overnight in a 24-well plate at 1.0 × 10<sup>5</sup> cells/well. During the ultrasound transfection, the microbubble concentration (MC) was 300 μL/mL, the plasmid concentration (PC) was 15 μg/mL, the ultrasound duration (ET) was 45 s, the ultrasound frequency was 1 MHz, and the load ratio was 20%. The ultrasound intensity (AI) was set to 0.5 W/cm<sup>2</sup>, 1.5 W/cm<sup>2</sup>, or 2.5 W/cm<sup>2</sup>. For specific steps, please refer to previous reports [15].

## Cell Grouping

The cells were divided into 5 groups: (1) untreated group: blank control without any treatment; (2) miR-21-EGFP plasmid group: treated with 15 µg miR-21-EGFP plasmid DNA; (3) miR-21-EGFP plasmid+UTMD 1.5 W/cm<sup>2</sup> group: ultrasonic exposure treatment with miR-21-EGFP plasmid plus PFPMS (AI 1.5 W/cm<sup>2</sup>, MC 300 µg/mL, PC 15 µg/mL, and ET 45 s); (4) miR-21 inhibitor-EGFP plasmid group: treated with 15 µg miR-21 inhibitor-EGFP plasmid DNA; (5) miR-21 inhibitor-EGFP plasmid+UTMD 1.5 W/cm<sup>2</sup> group: treated with miR-21 inhibitor-EGFP plasmid plus PFPMS for ultrasonic exposure (AI 1.5 W/cm<sup>2</sup>, MC 300 µg/mL, PC 15 µg/mL and ET 45 s). For ultrasound radiation, after adding a plasmid or transfection complex, we inserted a sterile ultrasound probe (Sonitron 2000V, NEPAGENE Japan, Chiba, Japan) directly into the bottom of the 24-well plate.

## Flow Cytometry

The transfection efficiency of the miR-21-EGFP and miR-21 inhibitor-EGFP plasmids was determined by flow cytometry after cell transfection in each group. First, transfected HeLa cells were collected using 0.25% trypsin-EDTA. Then, the concentration of the resuspended HeLa cells was adjusted to about 1×10<sup>6</sup> cells/mL. Finally, DNA transfection efficiency (number of cells expressing EGFP/total number of cells) was determined by evaluating EGFP expression using a flow cytometer at an excitation wavelength of 488 nm [15]. The kit was purchased from Beyotime (C1062S, Nantong, China). The simplified steps are as follows: Annexin V-FITC (5 µL, C1062M, Beyotime, Nantong, China) and propidium iodide staining solution (10 µL, PI, C1062M) were added to the cell suspension and the cells were incubated at room temperature in the dark for 10-20 min, then placed in an ice bath. Apoptosis was detected using a BD FACSCalibur flow cytometer (BD Biosciences, San Diego, CA, USA) and analyzed by BD CellQuest™ Pro Software version 5.1 (BD Biosciences, San Diego, CA, USA).

## Reverse Transcription Quantitative PCR

Cell lysis and total RNA extraction for each group were carried out using the TRIzol method at 4°C. The MicroRNA Reverse Transcription Kit (4366597, Thermo Fisher Scientific, Waltham, MA, USA) was used to detect the miRNA reverse transcription reaction. RT-qPCR was performed using the Verso 1-step RT-qPCR Kit (Thermo Fisher, Waltham, MA, USA) and RT-PCR detection system (ABI 7500, Life technology, Foster City, CA, USA). The relative expression levels were calculated using the 2<sup>-ΔΔCt</sup> method [16]. We used U6 as a housekeeping gene for miRNA, and β-actin as a housekeeping gene for mRNA. The primer sequences for the miR-21, Bax-F, Bcl-2, β-catenin, matrix metalloproteinase-9 (MMP-9), epidermal growth factor receptor (EGFR), β-actin, and U6 genes were as follows (5'-3'):

miR-21-F: TCATGGCAACACCAGTCGAT,  
miR-21-R: TATCCAGTGCCTGTCGTGG;  
AKT-F: AGCGACGTGGCTATTGTGAAG,  
AKT-R: GCCATCATTCTTGAGGAGGAAGT;  
Bax-F: CCCGAGAGGTCTTTTCCGAG,  
Bax-R: CCAGCCCATGATGGTCTGAT;  
Bcl-2-F: CCAGCGTATATCGGAATGTGG,  
Bcl-2-R: CCATGTGATACCTGCTGAGAAG;  
Wnt1-F: CGATGGTGGGGTATTGTGAAC,  
Wnt1-R: CCGGATTTGGCGTATCAGAC;  
β-catenin-F: CCTATGCAGGGGTGTCAAC,  
β-catenin-R: CGACCTGGAAAACGCCATCA;  
MMP-9-F: TGTACCGCTATGGTTACTCTCG,  
MMP-9-R: GGCAGGGACAGTTGCTTCT;  
EGFR-F: TTGCCGCAAAGTGTGTAACG,  
EGFR-R: GTCACCCCTAAATGCCACCG;  
β-actin-F: CATGTACGTTGCTATCCAGGC,  
β-actin-R: CTCCTTAATGTCACGCACGAT;  
U6-F: AAAGCAAATCATCGGACGACC,  
U6-R: GTACAACACATTGTTTCTCGGA.

## CCK-8 Assay

The density of HeLa cells was determined to be 1×10<sup>3</sup> cells/mL. Cells were seeded into a 96-well plate and pre-cultured for 24 h. After 48 h of incubation, 10 µL of CCK8 solution (HY-K0301, MedChemExpress, New Jersey, USA) was added to each well. After 2-4 h at 37°C, the absorbance at 450 nm was measured with a microplate reader (24072800, Thermo Scientific, Waltham, MA, USA).

## Wound Healing Assay

HeLa cells (8×10<sup>5</sup>) were seeded in a 6-well plate for 24 h. On the next day, we drew 2 parallel lines on the cell culture layer using a sterile pipette tip, we rinsed the floating cells with phosphate-buffered saline (PBS), and we placed them in the incubator for 24 h. Cell migration images were observed under a microscope (BZ-8100, Keyence, Itasca, IL, USA). Image-Pro Plus 4.1 analysis software (Media Cybernetics Company, Bethesda, MD, USA) was used to observe the distance of cell migration and to take images.

## Transwell Migration Assay

The invasion ability of the HeLa cells was determined using the transwell migration assay method (CLS3398, Sigma, Munich, Germany). The cells (4×10<sup>5</sup> cells/well) were seeded into the upper chamber with 200 mg/mL Matrigel (354230, BD, San Diego, CA, USA). Serum-free medium was added to the supernatant, and 20% serum medium was added to the lower chamber to form a nutrient concentration gradient, thereby promoting the transfer of cells to the lower chamber. After incubation for 24

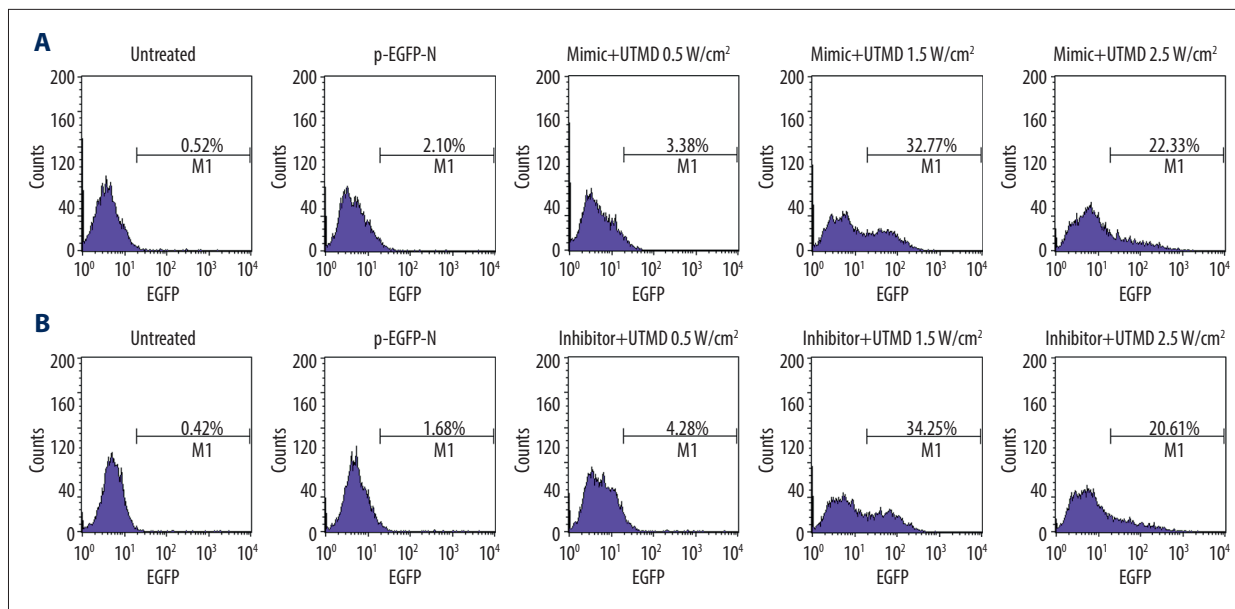


**Figure 1.** UTMD-mediated plasmid transfection of HeLa cells. **(A)** The influence of ultrasound intensity of 0.5 W/cm<sup>2</sup>, 1.5 W/cm<sup>2</sup>, and 2.5 W/cm<sup>2</sup> on the transfection rate of the miR-21-EGFP plasmid was determined by flow cytometry. **(B)** The effect of ultrasound intensity of 0.5 W/cm<sup>2</sup>, 1.5 W/cm<sup>2</sup>, and 2.5 W/cm<sup>2</sup> on the transfection efficiency of miR-21 inhibitor-EGFP plasmid was determined by flow cytometry. The microbubble concentration was 300 μL/mL, the plasmid concentration was 15 μg/mL, the ultrasound duration was 45 s, the ultrasound frequency was 1 MHz, and the load ratio was 20%. UTMD – ultrasound-targeted microbubble destruction; EGFP – enhanced green fluorescent protein.

h at 37°C, the cells that had invaded through the membrane were fixed with 4% paraformaldehyde and stained with 0.1% crystal violet for 20 min. For each group, 4 fields of view were counted. The number of cells per field was calculated using an inverted microscope.

### Western Blot Analysis

Total protein concentration was extracted from HeLa cells using a RIPA lysate (89901, Thermo Fisher Scientific, Waltham, MA, USA). Protein concentration was measured using a protein detection kit (A53227, Thermo Fisher Scientific, Waltham, MA, USA). A volume of 30 μg protein for each cell was transferred to a PVDF membrane (HVLPO4700, Millipore, Billerica, MA, USA) using the SDS-PAGE method. After the transfer was completed, the membrane was soaked from bottom to top with TBS, then placed in an incubation box containing a 5% skimmed milk powder solution (37°C, 1 h), incubated with shaking at room temperature on a decolorization shake flask for 2 hours, and then incubated with phosphorylated (p)-Akt (1: 1000; 56 KD; ab38449; Abcam, Cambridge, UK), Akt (1: 500; 55 KD; ab8805), Bax (1: 1000; 21 KD; ab32503), Bcl-2 (1: 1000; 26 KD; ab59348), Wnt1 (1 μg/mL; 41 KD; ab85060), MMP-9 (1 μg/mL; 95 KD; ab73734), EGFR (1: 1000; 134 KD; ab52894), β-catenin (1: 1000; 92 KD; #9562; Cell signaling technology, Danvers, MA, USA), or β-actin (1: 1000; 45 KD; #4970) overnight at 4°C. The target band was incubated with

a goat anti-rabbit IgG H&L (HRP) (1: 5000; ab205718; Abcam, Cambridge, UK) for 2 h. Finally, the signals were detected using SignalFir ECL reagent (#6883) and the gray value of the band was analyzed and calculated using ImageJ (version 5.0, Bio-Rad, Hercules, CA, USA) [17].

### Statistical Analysis

Values were expressed as mean±SD. The data were analyzed by *t* test using Statistical Software Prism 7 (GraphPad Software, Inc., San Diego, CA, USA) following one-way analysis of variance (ANOVA). Bonferroni adjustment was applied for comparison of multiple groups (≥3). *P*<0.05 was considered statistically significant.

## Results

### Effects of UTMD with Different Ultrasound Intensities on the Transfection Efficiency of miR-21

In order to determine the optimal ultrasound intensity parameters for UTMD-transfection of HeLa cells, the UTMD-mediated miR-21-EGFP plasmid transfection was quantitatively analyzed by flow cytometry for 48 h. The results showed that when the ultrasound intensity was 1.5 W/cm<sup>2</sup>, the fluorescence intensity was the highest and the transfection effect was the

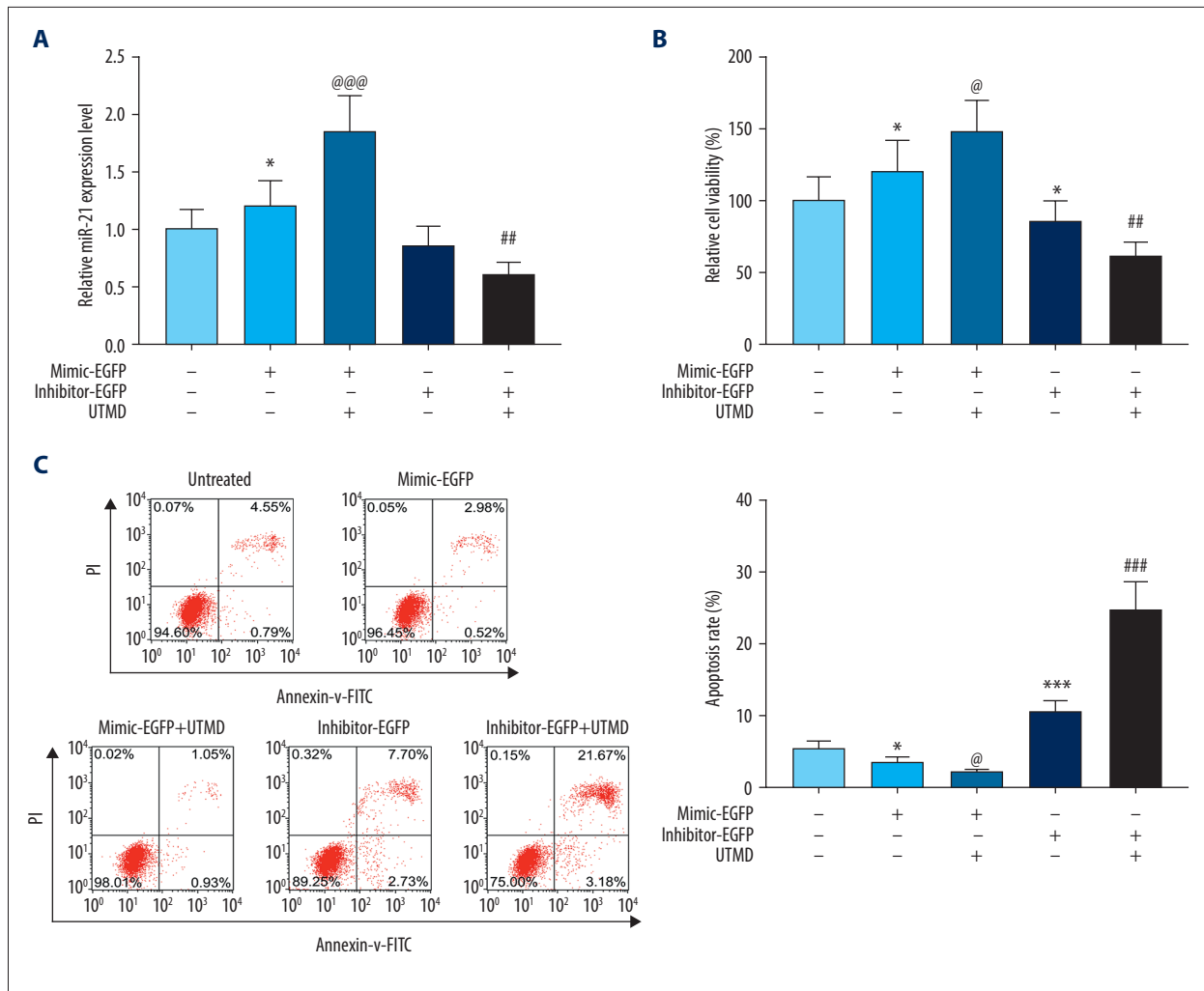


**Figure 2.** Effects of UTMD-mediated miR-21 transfection on HeLa cell viability and apoptosis. **(A)** RT-qPCR was used to determine the expression of miR-21 in the untreated, mimic-EGFP, mimic-EGFP+UTMD, inhibitor-EGFP, and inhibitor-EGFP+UTMD groups. U6 was used as an internal reference. The ultrasonic intensity was 1.5 W/cm<sup>2</sup>. **(B)** CCK-8 was used to detect the effect of miR-21 plasmid on the survival rate of HeLa cells (ultrasonic intensity was 1.5 W/cm<sup>2</sup>). **(C)** The effect of miR-21 plasmid on the apoptosis rate of HeLa cells was selected by flow cytometry (ultrasonic intensity was 1.5 W/cm<sup>2</sup>). \*  $P < 0.05$  and \*\*\*  $P < 0.001$  vs untreated; @  $P < 0.05$  and @@@  $P < 0.001$  vs mimic+EGFP; ##  $P < 0.01$  and ###  $P < 0.001$  vs inhibitor+EGFP. UTMD – ultrasound-targeted microbubble destruction; RT-qPCR – reverse transcription quantitative polymerase chain reaction; EGFP – enhanced green fluorescent protein.

best (Figure 1A). To further determine whether this ultrasound intensity was suitable for miR-21 inhibitor-EGFP plasmid transfection, the fluorescence intensity of the untreated, pEGFP-N, inhibitor+UTMD 0.5 W/cm<sup>2</sup>, inhibitor+UTMD 1.5 W/cm<sup>2</sup>, inhibitor+UTMD 2.5 W/cm<sup>2</sup> groups were compared and analyzed by flow cytometry. The results showed that the miR-21 inhibitor-EGFP plasmid+UTMD 1.5 W/cm<sup>2</sup> group had the highest fluorescence intensity, indicating that the transfection effect was the best at 1.5 W/cm<sup>2</sup> ultrasound intensity (Figure 1B). Therefore, the following experiments were performed based on 1.5 W/cm<sup>2</sup> ultrasound intensity.

### Effect of UTMD-mediated miR-21 Plasmid on HeLa Cell Proliferation and Apoptosis

The mRNA level of miR-21 in HeLa cells under different treatment conditions was detected by RT-PCR. Compared with the untreated group, the expression of miR-21 in the miR-21-EGFP plasmid group was significantly increased, and after UTMD treatment, the expression level of miR-21 was extremely and significantly higher than that of the miR-21-EGFP plasmid group ( $P < 0.05$ , Figure 2A). Compared with the miR-21 inhibitor-EGFP plasmid group, the miR-21 expression in the miR-21 inhibitor-EGFP plasmid+UTMD group was significantly



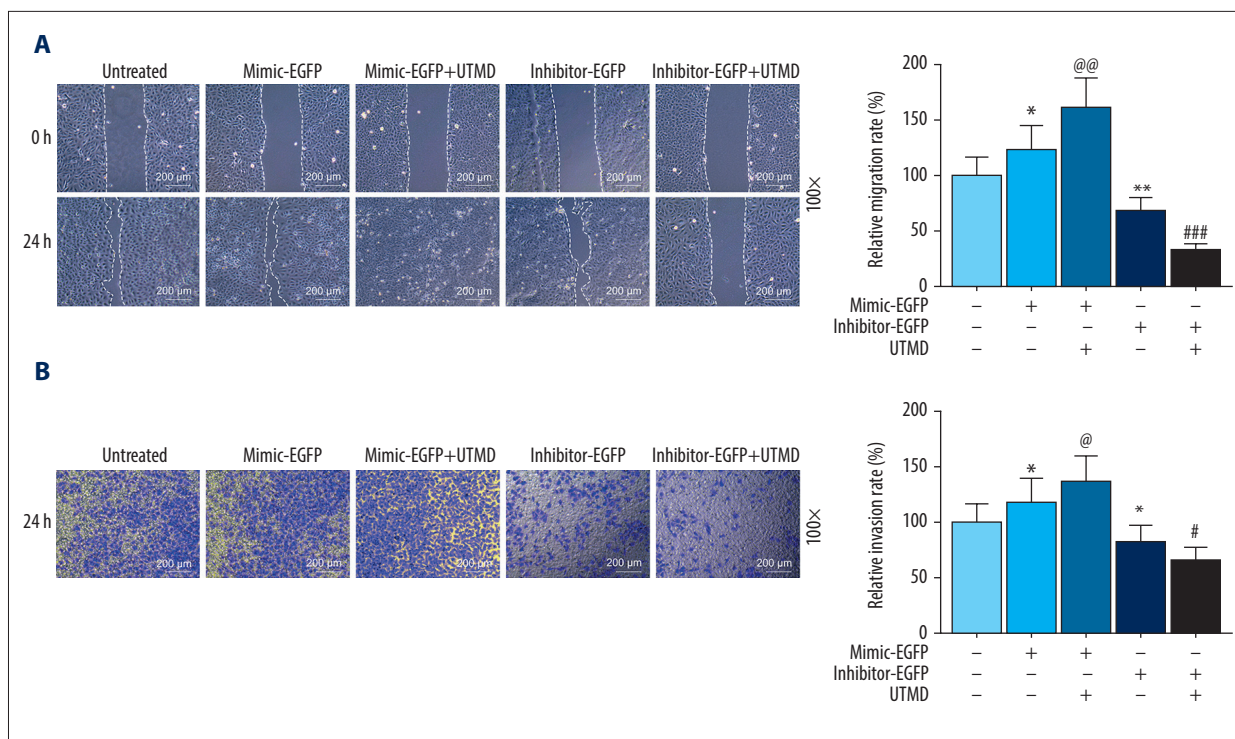


**Figure 3.** Effects of UTMD-mediated miR-21 transfection on HeLa cell migration and invasion. **(A)** Wound healing experiments were performed to detect the effects of miR-21 plasmid on HeLa cell migration in the untreated, mimic-EGFP, mimic-EGFP+UTMD, inhibitor-EGFP, and inhibitor-EGFP+UTMD groups (ultrasonic intensity was 1.5 W/cm<sup>2</sup>). **(B)** The transwell migration assay was used to detect the effect of the miR-21 plasmid on HeLa cell invasion (ultrasonic intensity was 1.5 W/cm<sup>2</sup>). UTMD: Ultrasound-targeted microbubble destruction; EGFP: enhanced green fluorescent protein. \* *P*<0.05 and \*\* *P*<0.01 vs untreated; @ *P*<0.05 and @@ *P*<0.01 vs mimic+EGFP; # *P*<0.05 and ### *P*<0.001 vs inhibitor+EGFP. UTMD – ultrasound-targeted microbubble destruction; EGFP – enhanced green fluorescent protein.

reduced (*P*<0.05, **Figure 2A**). CCK8 results showed that the miR-21-EGFP plasmid+UTMD group had a more significant effect on promoting cell viability than the miR-21-EGFP plasmid group (*P*<0.05, **Figure 2B**). The UTMD-mediated miR-21 inhibitor-EGFP group inhibited cell viability more than the simple miR-21 inhibitor-EGFP plasmid treatment group (*P*<0.05, **Figure 2B**). Flow cytometry was used to further examine the effect of the UTMD-mediated miR-21 plasmid on HeLa cell apoptosis, and found that the apoptosis rate in the miR-21-EGFP plasmid+UTMD group was significantly lower than that in the miR-21-EGFP plasmid group (*P*<0.05, **Figure 2C**). In addition, the inhibitor-EGFP plasmid+UTMD group had a significantly higher apoptosis rate than the inhibitor-EGFP plasmid group (*P*<0.05, **Figure 2C**).

**Effect of UTMD-mediated miR-21 Plasmid on HeLa Cell Migration and Invasion**

To further investigate the effects of UTMD-mediated miR-21 transfection on the biological effects of HeLa cells, wound healing experiments and transwell migration assay experiments were used in this study. As shown in **Figure 3A**, the miR-21-EGFP

plasmid+UTMD group had a significantly higher migration rate than the miR-21-EGFP plasmid group (*P*<0.05). The inhibitor-EGFP plasmid+UTMD group had a significantly lower migration rate than the inhibitor-EGFP plasmid group (*P*<0.05, **Figure 3A**). In addition, invasion experiments also indicated that miR-21 mediated by UTMD has more obvious effects on HeLa cells. The miR-21-EGFP plasmid+UTMD group had a significantly higher invasion rate than the miR-21-EGFP plasmid group (*P*<0.05, **Figure 3B**). The inhibitor-EGFP plasmid+UTMD group had a significantly lower invasion rate than the inhibitor-EGFP plasmid group (*P*<0.05, **Figure 3B**).

**Effects of UTMD-mediated miR-21 on Apoptosis, Metastasis, and Wnt/Akt Pathway-related Genes**

In order to investigate the mechanism of UTMD-mediated miR-21 transfection on HeLa cells, western blot was used to detect the effect of the miR-21 plasmid on apoptosis, metastasis, and Wnt/Akt pathway-related genes. The results showed that, compared with the untreated group, the expression levels of p-Akt, Akt, Bcl-2, Wnt, β-catenin, MMP-9, and EGFR in the miR-21-EGFP plasmid group were significantly increased,

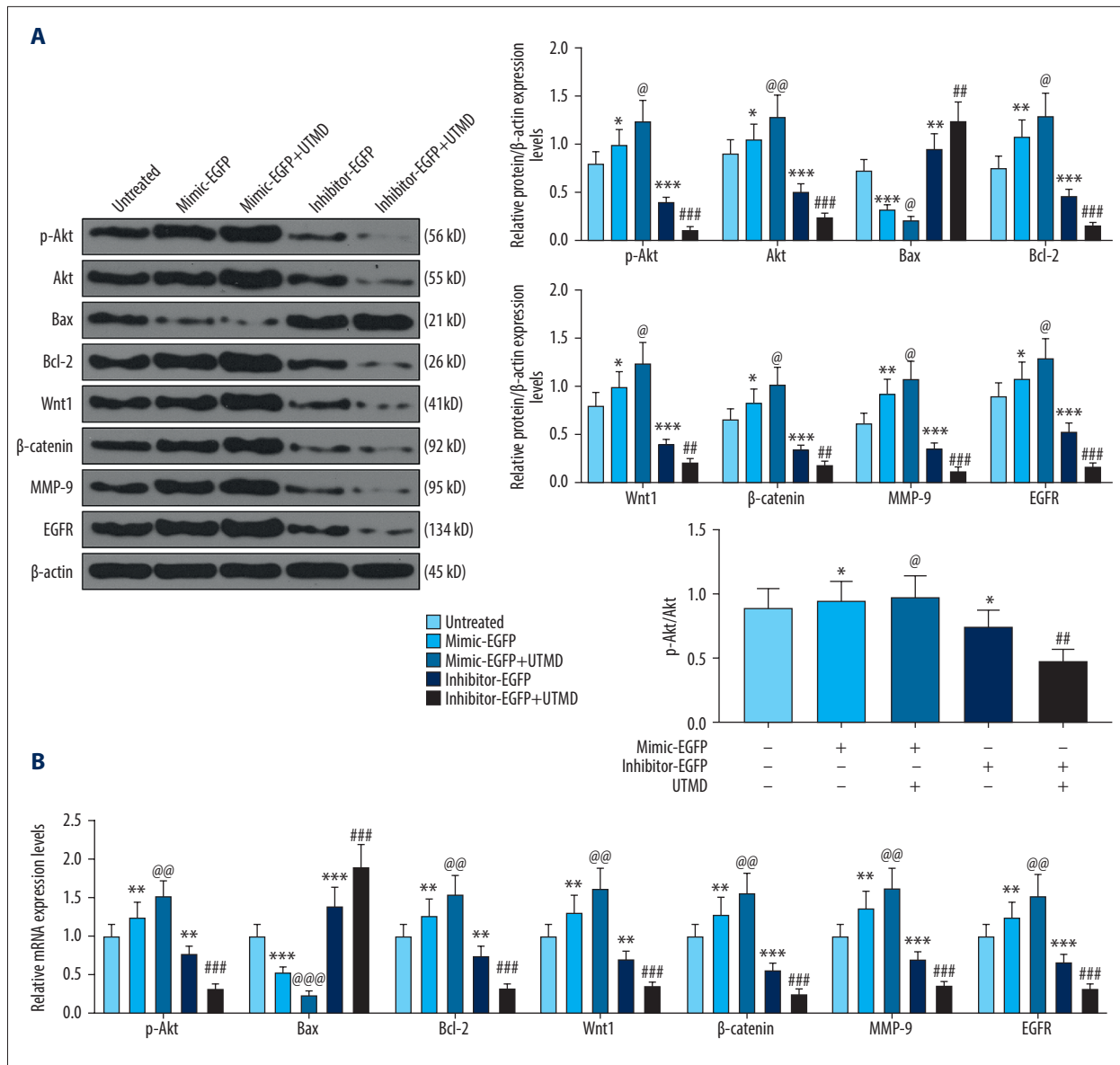


**Figure 4.** Effects of UTMD-mediated miR-21 transfection on apoptosis, metastasis, and Wnt/Akt pathway-related genes. **(A)** Western blot was used to detect the effects of the miR-21 plasmid on phosphorylated (p)-Akt, Akt, Bax, Bcl-2, Wnt, β-catenin, MMP-9, and EGFR expression in HeLa cells; β-actin was an internal reference (ultrasonic intensity of 1.5 W/cm<sup>2</sup>). **(B)** RT-qPCR was used to detect the effects of miR-21 plasmid on Akt, Bax, Bcl-2, Wnt, β-catenin, MMP-9, and EGFR expression in HeLa cells; β-actin was an internal reference (ultrasonic intensity of 1.5 W/cm<sup>2</sup>). \*  $P < 0.05$ , \*\*  $P < 0.01$ , and \*\*\*  $P < 0.001$  vs untreated; @  $P < 0.05$ , @@  $P < 0.01$  and @@@  $P < 0.001$  vs mimic+EGFP; #  $P < 0.01$  and ###  $P < 0.001$  vs inhibitor+EGFP. UTMD – ultrasound-targeted microbubble destruction; RT-qPCR – reverse transcription quantitative polymerase chain reaction; EGFR – epidermal growth factor receptor; EGFP – enhanced green fluorescent protein.

and Bax expression was significantly decreased. However, the increase in expression conferred by miR-21 was more significant after UTMD mediation ( $P < 0.05$ , **Figure 4A**). Similarly, compared with the miR-21 inhibitor-EGFP plasmid group, p-Akt, Akt, Bcl-2, Wnt, β-catenin, MMP-9, and EGFR expression in the miR-21 inhibitor-EGFP plasmid+UTMD group significantly decreased, while Bax expression significantly increased ( $P < 0.05$ ,

**Figure 4A**). In addition, the results of RT-qPCR further verified that UTMD-mediated cells experienced enhanced miR-21 function. After UTMD, the expressions of Akt, Bax, Bcl-2, Wnt, β-catenin, MMP-9, and EGFR in the miR-21-EGFP plasmid group and miR-21 inhibitor-EGFP plasmid group increased or decreased significantly ( $P < 0.05$ , **Figure 4B**).

## Discussion

In cervical cancer, abnormal expression of precancerous miRNAs and tumor suppressor miRNAs is necessary for cancer cell growth [18]. Studies have shown that miR-21 can promote the occurrence and development of breast cancer, cervical cancer, and liver cancer [19-22]. In the present study, miR-21-EGFP and miR-21 inhibitor-EGFP were transfected in HeLa cells. It was also found that upregulation of miR-21 can promote cell proliferation, migration, and invasion, and can inhibit apoptosis, in HeLa cells. Blocking miR-21 expression can significantly inhibit cell growth and induce apoptosis. This is highly consistent with related reports, suggesting that miR-21 plays an important role in the pathogenesis of cervical cancer and may become an important target for cervical cancer gene therapy.

Related studies at home and abroad have reported that ultrasound microbubbles can enhance the transfection efficiency of genes on retinoblastoma cells, liver cells, and myocardial cells [23-25]. Although there have been reports on the optimization of ultrasound microbubble conditions, their optimization parameters were not standardized [26]. In the present experiment, when the cells were transfected with miR-21-EGFP and miR-21 inhibitor-EGFP, the intensity of ultrasound was measured. The results showed that the intensity of 1.5 W/cm<sup>2</sup> ultrasound is the optimal transfection parameter for this study, laying a foundation for subsequent experiments. The transfection efficiency at the ultrasound intensity of 2.5 W/cm<sup>2</sup> is lower than that of the 1.5 W/cm<sup>2</sup> ultrasound intensity. The reason may be that when the ultrasound intensity reaches a certain level, it might cause irreversible damage to the cells and cause a decrease in transfection efficiency. Ultrasound irradiation can not only promote the transfection of genes; the "blast" produced by the ultrasound combined with the microbubble contrast agents can also improve the transfection efficiency for the target gene [8,15]. In an in vitro experiment with HeLa (cervical cancer) cells, we compared the effects of UTMD-mediated miR-21 plasmid and simple miR-21 plasmid treatment on cell biology, and found that the effects of miR-21-EGFP and miR-21 inhibitor-EGFP on HeLa cells were more obvious after UTMD treatment, including effects on cell proliferation, migration, invasion, and apoptosis, which further supports the idea that UTMD can enhance the transfection rate and expression of genes.

Several studies have found that many signaling pathways are involved in the development of cervical cancer, such as ERK/MAPK, PI3K/Akt, EGFR/VEGFR, apoptosis, and Wnt1/β-catenin [27-30]. One important marker that affects the cell cycle, cell proliferation, and resistance to apoptosis is p-Akt/Akt [31]. Bcl-2 is an apoptosis-inhibiting gene, and Bax not only antagonizes the inhibitory effect of Bcl-2, but also has the function of promoting apoptosis [32,33]. The abnormal activation of the Wnt/β-catenin pathway may promote tumor progression by stimulating the proliferation of cancer cells through cyclinD1/c-myc [34,35]. MMP-9 is a member of the matrix metalloproteinase family, which can reshape and degrade the homeostasis of the extracellular matrix [36]. EGFR overexpression is related to the development of cervical cancer and plays an important role in the process of cancer cell proliferation and metastasis [29]. In the present study, several related proteins were selected and tested. The results indicate that miR-21 may participate in the regulation of cervical cancer by participating in the regulation of different signaling pathways, such as the Akt, EGFR, and Wnt1/β-catenin pathways, and that UTMD significantly enhances the regulatory effect of miR-21 on downstream pathways.

It would be beneficial to perform more experiments related to the correlation between miR-21 and the Wnt/Akt pathway, as well as in vivo experiments, in future studies. The lack of these were limitations of this study.

## Conclusions

In summary, 1.5 W/cm<sup>2</sup> ultrasound UTMD can effectively promote the transfection of exogenous miR-21 into HeLa cells, a cell line derived from cervical cancer cells, and enhance the expression and function of the miR-21 gene in HeLa cells. It can also intensify the effect of miR-21 on apoptosis, metastasis, and phosphorylation genes in cervical cancer cells.

## Conflict of Interest

None.



## References:

1. Li H, Wu X, Cheng X. Advances in diagnosis and treatment of metastatic cervical cancer. *J Gynecol Oncol*, 2016;27(4):e43
2. Lim MC, Won YJ, Lim J, et al. Second primary cancer after diagnosis and treatment of cervical cancer. *Cancer Res Treat*, 2016;48(2):641-49
3. Cadron I, Van Gorp T, Amant F, et al. Chemotherapy for recurrent cervical cancer. *Gynecol Oncol*, 2007;107(1 Suppl. 1):S113-18
4. Angioli R, Plotti F, Montera R, et al. Neoadjuvant chemotherapy plus radical surgery followed by chemotherapy in locally advanced cervical cancer. *Gynecol Oncol*, 2012;127(2):290-96
5. Regalado Porras GO, Chavez Noguera J, Poitevin Chacon A. Chemotherapy and molecular therapy in cervical cancer. *Rep Pract Oncol Radiother*, 2018;23(6):533-39
6. Bentivegna E, Gouy S, Maulard A, et al. Oncological outcomes after fertility-sparing surgery for cervical cancer. A systematic review. *Lancet Oncol*, 2016;17(6):e240-53
7. Chen S, Grayburn PA. Ultrasound-targeted microbubble destruction for cardiac gene delivery. *Methods Mol Biol*, 2017;1521:205-18
8. heng KT. Perflutren lipid microspheres. *Molecular Imaging and Contrast Agent Database (MICAD) website*. Bethesda (MD) 2004, <https://www.ncbi.nlm.nih.gov/books/NBK25377/>
9. Wu J, Li RK. Ultrasound-targeted microbubble destruction in gene therapy: A new tool to cure human diseases. *Genes Dis*, 2017;4(2):64-74
10. Chen H, Hwang JH. Ultrasound-targeted microbubble destruction for chemotherapeutic drug delivery to solid tumors. *J Ther Ultrasound*, 2013;1:10
11. Dimceviski G, Kotopoulos S, Bjanec T, et al. A human clinical trial using ultrasound and microbubbles to enhance gemcitabine treatment of inoperable pancreatic cancer. *J Control Release*, 2016;243:172-81
12. Han Y, Xu GX, Lu H, et al. Dysregulation of miRNA-21 and their potential as biomarkers for the diagnosis of cervical cancer. *Int J Clin Exp Pathol*, 2015;8(6):7131-39
13. Zhang Z, Wang J, Wang X, et al. MicroRNA-21 promotes proliferation, migration, and invasion of cervical cancer through targeting TIMP3. *Arch Gynecol Obstet*, 2018;297(2):433-42
14. Liu Y, Li L, Su Q, et al. Ultrasound-targeted microbubble destruction enhances gene expression of microRNA-21 in swine heart via intracoronary delivery. *Echocardiography (Mount Kisco, NY)*, 2015;32(9):1407-16
15. Zhang L, Sun Z, Ren P, et al. Ultrasound-targeted microbubble destruction (UTMD) assisted delivery of shRNA against PHD2 into H9C2 cells. *PLoS One*, 2015;10(8):e0134629
16. Singh C, Roy-Chowdhuri S. Quantitative real-time PCR: Recent advances. *Methods Mol Biol*, 2016;1392:161-76
17. Kurien BT, Scofield RH. Western blotting: an introduction. *Methods Mol Biol*, 2015;1312:17-30
18. Li J, Liu Q, Clark LH, et al. Deregulated miRNAs in human cervical cancer: Functional importance and potential clinical use. *Future Oncol*, 2017;13(8):743-53
19. Jazbutyte V, Thum T. MicroRNA-21: From cancer to cardiovascular disease. *Curr Drug Targets*, 2010;11(8):926-35
20. Jiang J, Yang P, Guo Z, et al. Overexpression of microRNA-21 strengthens stem cell-like characteristics in a hepatocellular carcinoma cell line. *World J Surg Oncol*, 2016;14(1):278
21. Yao T, Lin Z. MiR-21 is involved in cervical squamous cell tumorigenesis and regulates CCL20. *Biochim Biophys Acta*, 2012;1822(2):248-60
22. Xu J, Zhang W, Lv Q, Zhu D. Overexpression of miR-21 promotes the proliferation and migration of cervical cancer cells via the inhibition of PTEN. *Oncol Rep*, 2015;33(6):3108-16
23. Luo J, Zhou X, Diao L, Wang Z. Experimental research on wild-type p53 plasmid transfected into retinoblastoma cells and tissues using an ultrasound microbubble intensifier. *J Int Med Res*, 2010;38(3):1005-15
24. Zhao DW, Tian M, Yang JZ, et al. Hemostatic mechanism underlying microbubble-enhanced non-focused ultrasound in the treatment of a rabbit liver trauma model. *Exp Biol Med (Maywood)*, 2017;242(2):231-40
25. Chang X, Liu J, Liao X, Liu G. Ultrasound-mediated microbubble destruction enhances the therapeutic effect of intracoronary transplantation of bone marrow stem cells on myocardial infarction. *Int J Clin Exp Pathol*, 2015;8(2):2221-34
26. Guo X, Guo S, Pan L, et al. Anti-microRNA-21/221 and microRNA-199a transfected by ultrasound microbubbles induces the apoptosis of human hepatoma HepG2 cells. *Oncol Lett*, 2017;13(5):3669-75
27. Bahrami A, Hasanzadeh M, Hassanian SM, et al. The potential value of the PI3K/Akt/mTOR signaling pathway for assessing prognosis in cervical cancer and as a target for therapy. *J Cell Biochem*, 2017;118(12):4163-69
28. Yang M, Wang M, Li X, et al. The role of lncRNAs in signaling pathway implicated in CC. *J Cell Biochem*, 2019;120(3):2703-12
29. Li H, Lu Y, Pang Y, et al. Propofol enhances the cisplatin-induced apoptosis on cervical cancer cells via EGFR/JAK2/STAT3 pathway. *Biomed Pharmacother*, 2017;86:324-33
30. Ramachandran I, Thavathiru E, Ramalingam S, et al. Wnt inhibitory factor 1 induces apoptosis and inhibits cervical cancer growth, invasion and angiogenesis in vivo. *Oncogene*, 2012;31(22):2725-37
31. Zheng J, Dai X, Chen H, et al. Down-regulation of LHPP in cervical cancer influences cell proliferation, metastasis and apoptosis by modulating AKT. *Biochem Biophys Res Commun*, 2018;503(2):1108-14
32. Chen XF, Liu Y. MicroRNA-744 inhibited cervical cancer growth and progression through apoptosis induction by regulating Bcl-2. *Biomed Pharmacother*, 2016;81:379-87
33. Jiang Y, Xu H, Wang J. Alantolactone induces apoptosis of human cervical cancer cells via reactive oxygen species generation, glutathione depletion and inhibition of the Bcl-2/Bax signaling pathway. *Oncol Lett*, 2016;11(6):4203-7
34. Lan K, Zhao Y, Fan Y, et al. Sulfiredoxin may promote cervical cancer metastasis via Wnt/beta-catenin signaling pathway. *Int J Mol Sci*, 2017;18(5):917
35. Wu Y, Wang A, Zhu B, et al. KIF18B promotes tumor progression through activating the Wnt/beta-catenin pathway in cervical cancer. *Onco Targets Ther*, 2018;11:1707-20
36. Fan D, Wang Y, Qi P, et al. MicroRNA-183 functions as the tumor suppressor via inhibiting cellular invasion and metastasis by targeting MMP-9 in cervical cancer. *Gynecol Oncol*, 2016;141(1):166-74